The First XBT Science Workshop
" Building a Multi-Decadal Upper Ocean Temperature Record "

7-8 July, 2011, Melbourne, Australia

Basin Patterns of the upper ocean warming for 1993-2008

You-Soon Chang, Antony Rosati, Shaoqing Zhang, Gabriel Vecchi, Thomas Delworth, and Andrew Wittenberg

Gophysical Fluid Dynamics Laboratory / NOAA

Introduction

Lyman et al (2010, Nature) show a robust warming signal of the global upper ocean (0-700m).

They considered several sources of uncertainty associated with XBT correction and mapping method, which contributes to the differences among heat content estimations.

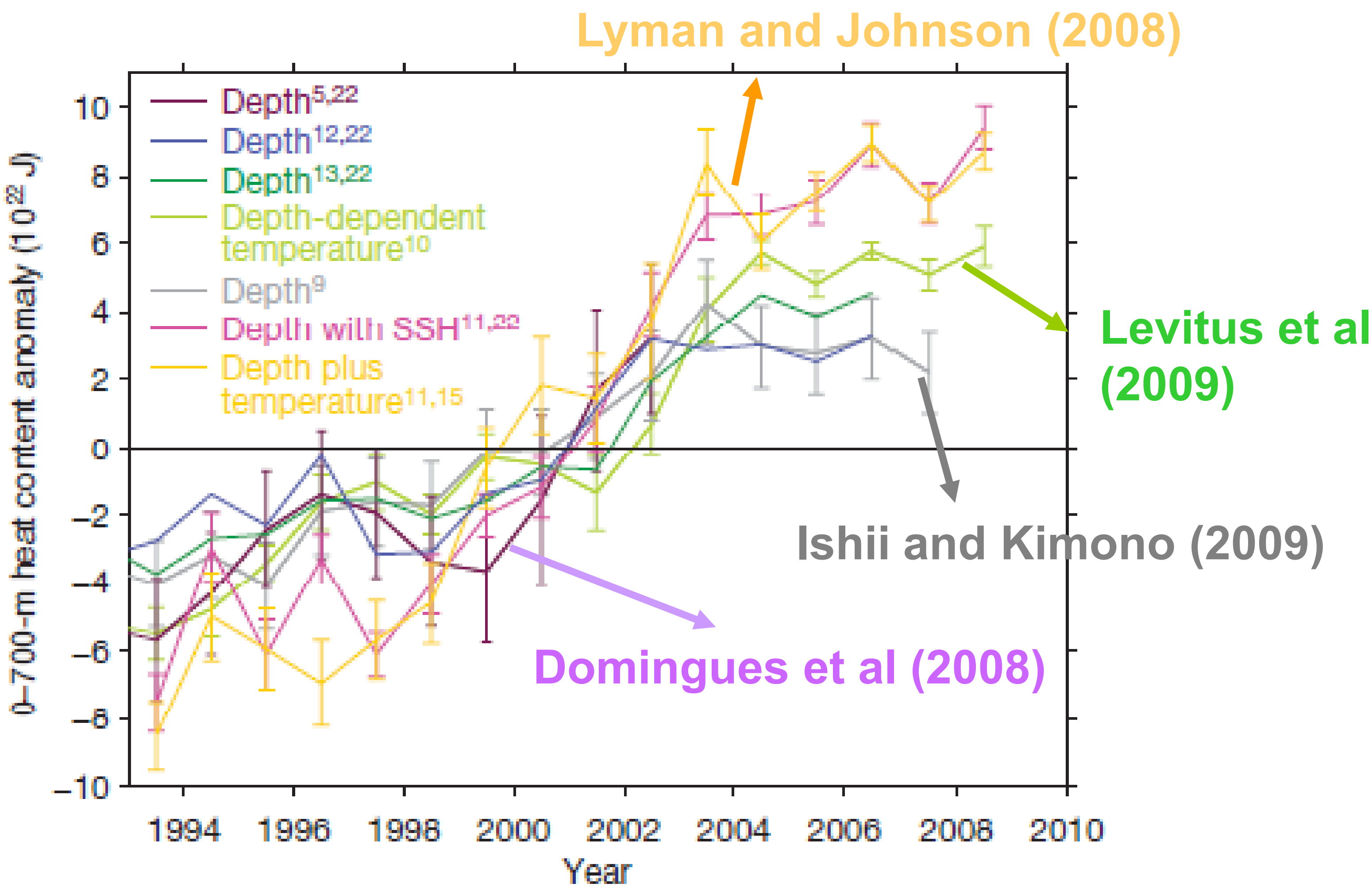

Introduction

- However, their focus is only limited in the globally averaged estimation. Warming trend is not uniform for the Global Ocean.
- Here, we present the spatial pattern of the global heat content change for 1993-2008.
- We also revisit the remaining issues for the global heat content patterns (e.g., rapid increasing pattern during the data transition periods from XBT to Argo, and the contribution of deep ocean warming to the upper ocean heat contents).

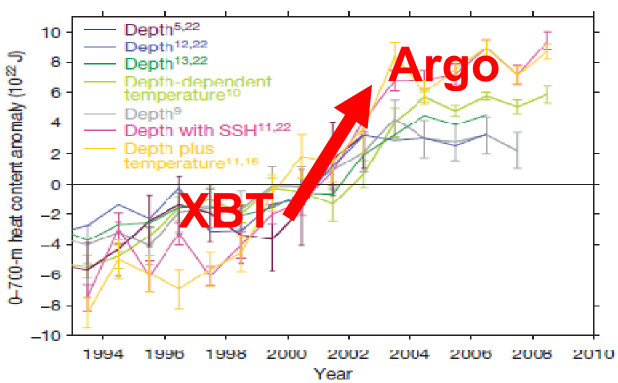

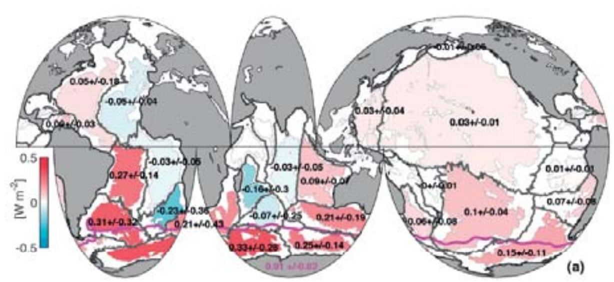

Purkey and Johnson, 2010

- Lastly, we present the preliminary results showing the impact of XBTs on the GFDL's ensemble coupled data assimilation system.

Part 1: Data Analysis for HC700

Data:

- Levitus09 (gridded (1 x 1 x yearly) heat contents (Levitus et al., 2009))
- WOD09 (in situ T,S profiles (NODC World Ocean Database 2009))
- Monthly net heat flux at TOA from NCEP2
- EN3 (gridded (1 x 1 x 42 levels X monthly) T, S fields)

Method:

- Global mean time series
- Spatial linear trend
- EOF analysis with ENSO signal removed

Global mean time series and linear trend for HC700

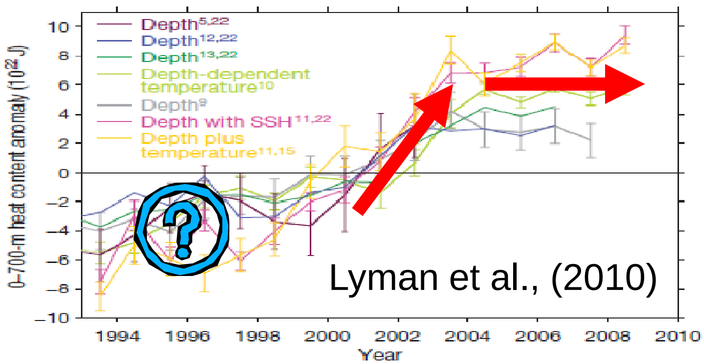

Warming areas: Western Pacific, Atlantic, Indian Ocean…

Cooling areas: Eastern Pacific, Gulf stream path…

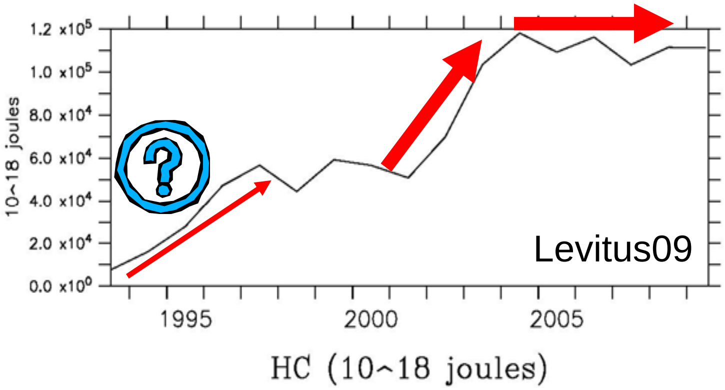

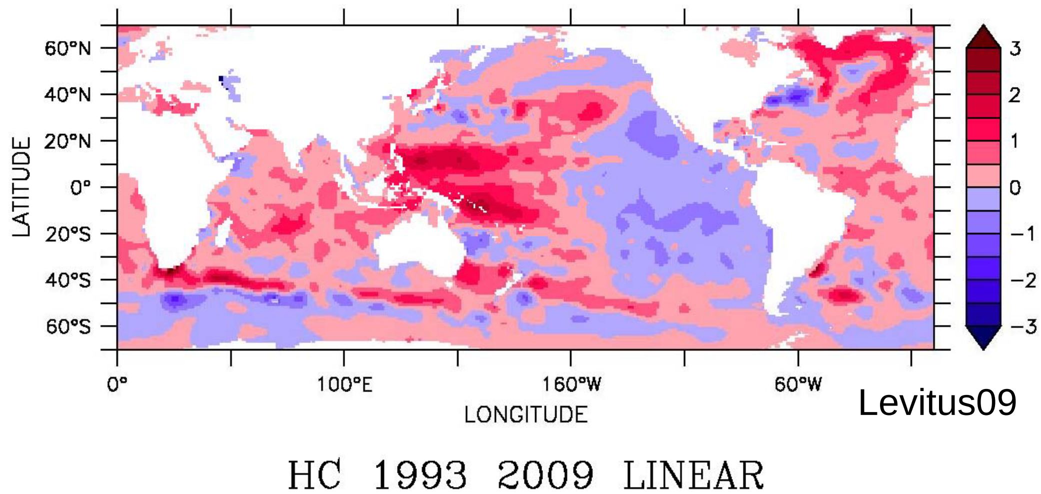

Time series of HC700 show three characteristics as below:

1. There are differences among the curves before 2000 (cooling, warming, no change). Levitus09 used in this study shows warming trend during these period.
2. All rapid increasing around 2000-2004.
3. All flatten out after around 2004.

Q1: HC700 is related to the no. obs (0-700m) ?

Levitus09 HC700

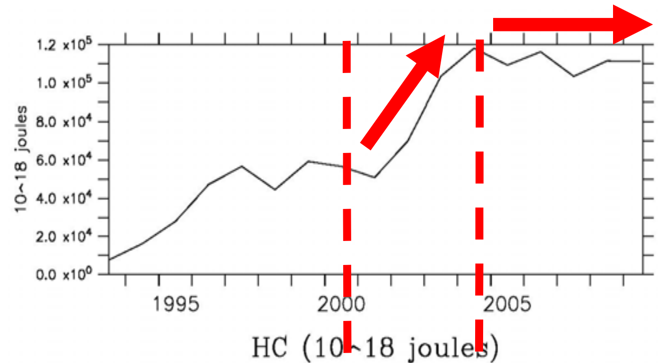

WOD09 (raw)

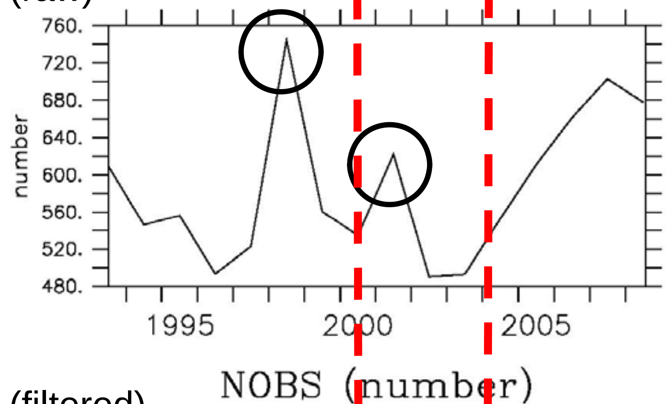

WOD09 (filtered)

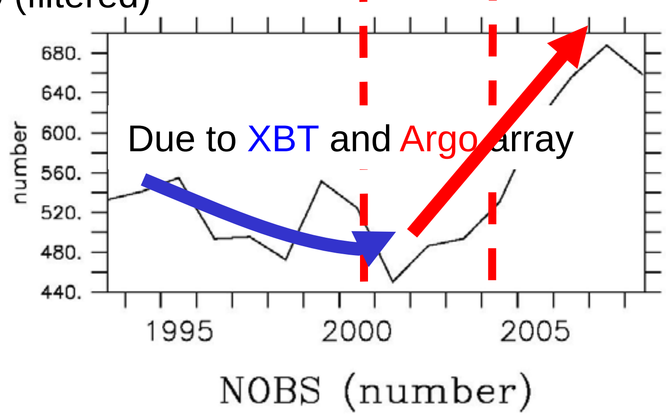

We calculate the number of observations (WOD09) after binning into 3 x 3 x 0-700m x 1 year.

There are high freq. datasets in 1998 and 2001 around the coastal areas obtained by intensive CTD observation projects during these years. So, we remove the grid box that the total number is not within the 3 sigma range.

No significant change related to the HC700 around 2000-2004 and after 2005.

WOD09 (XBT)

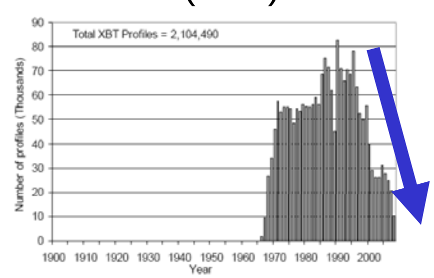

Figure 4.1. Temporal distribution of Expendable Bathythermograph (XBT) profiles in WOD09.

WOD09 (PFL-Argo)

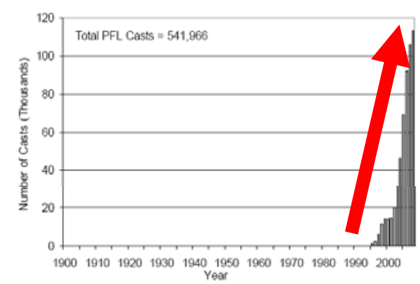

Figure 6.5. Temporal distributions of Profiling Float Data (PFL) casts in WOD09.

Q1: HC700 is related to the no. obs (0-700m) ?

Levitus09 HC700 linear trend

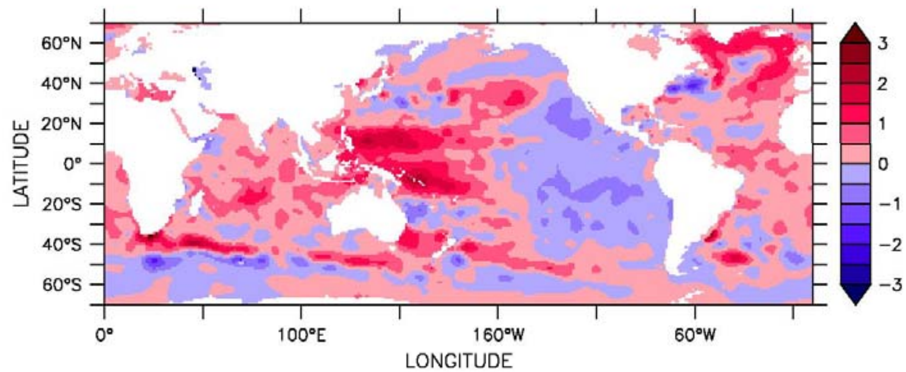

HC_1993_2009_LINEAR

WOD09 (raw) no. data linear trend

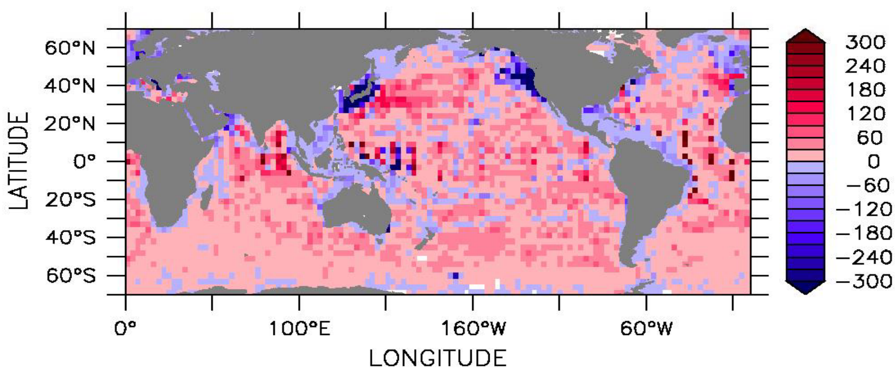

NOBS_1993_2008_LINEAR

WOD09 (filtered) no. data linear trend

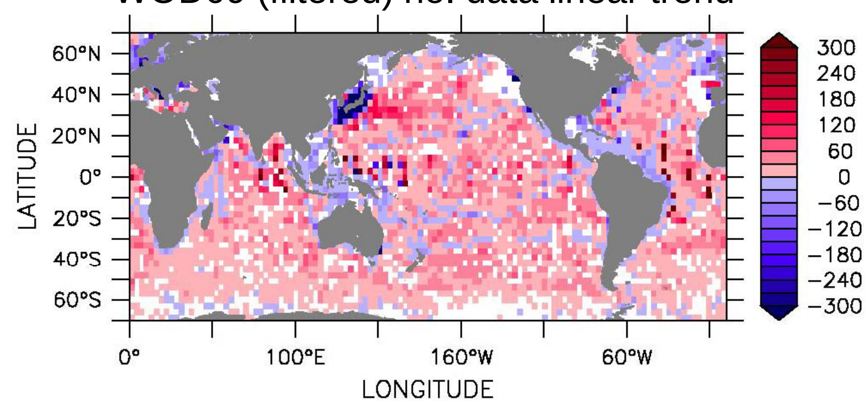

NOBS_1993_2008_LINEAR

There is no relationship of the spatial linear patterns.
Most oceans show increasing pattern of the number of data due to Argo array since 2000.

Q1: HC700 is related to the no. obs (700m-2000m) ?

Levitus09 HC700

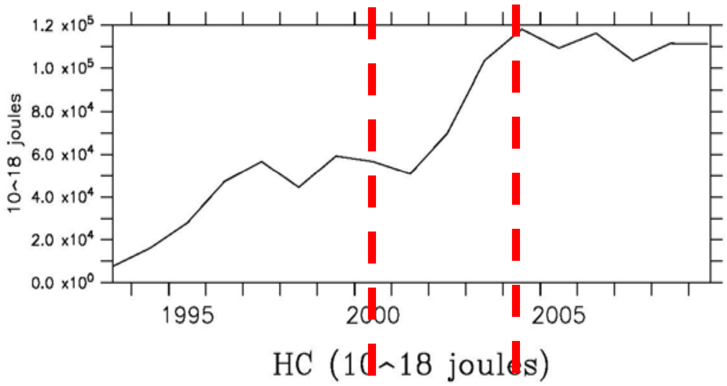

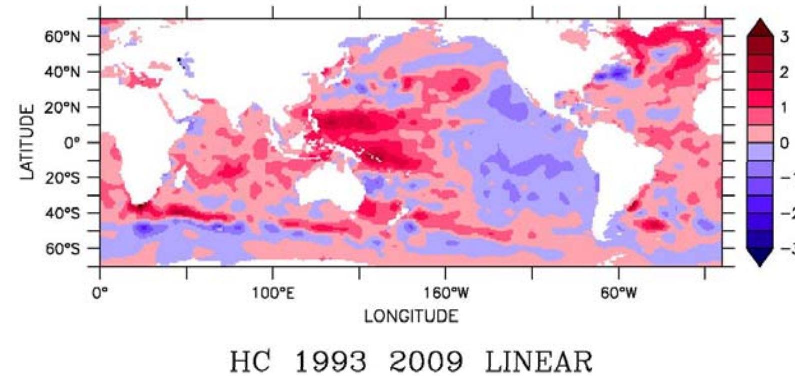

WOD09 (filtered)

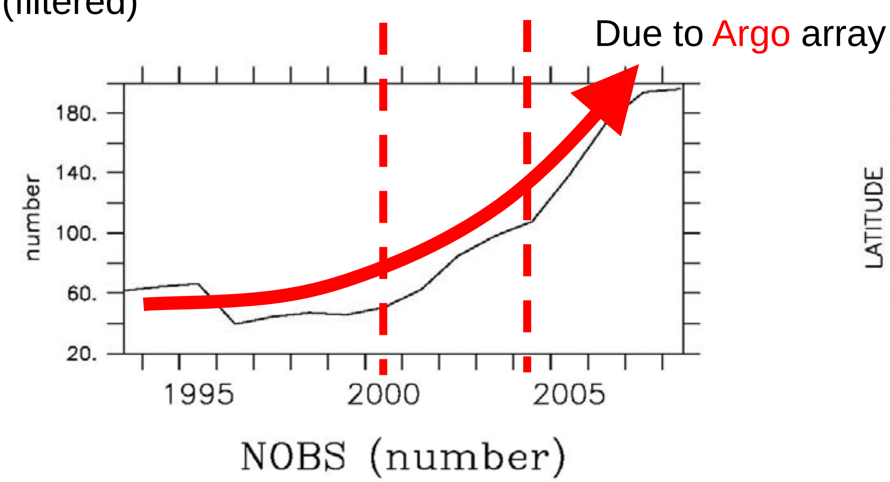

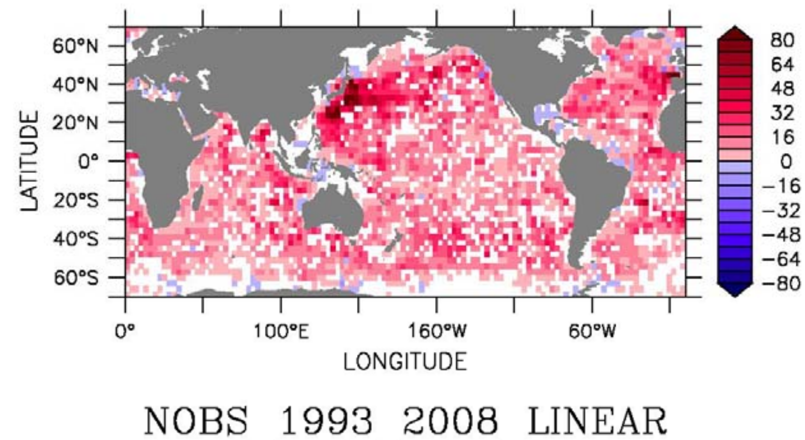

Increasing pattern from only Argo array.
No relationship between two time series and spatial patterns.

Q1: HC700 is related to the no. obs (2000m-5000m) ?

Levitus09 HC700

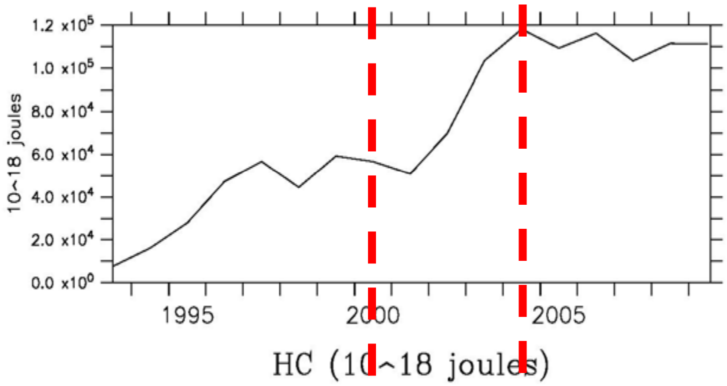

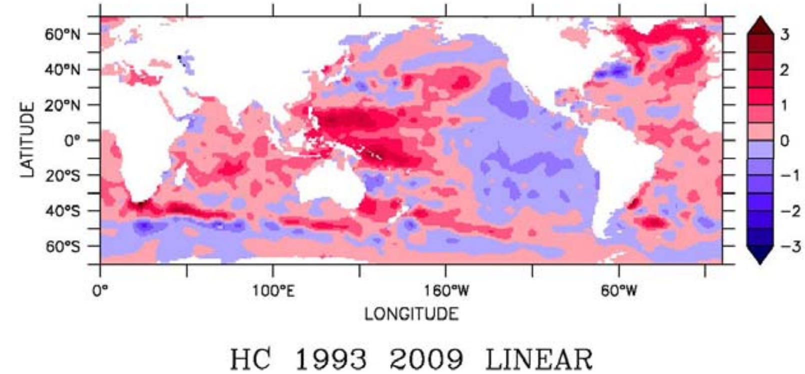

WOD09 (filtered)

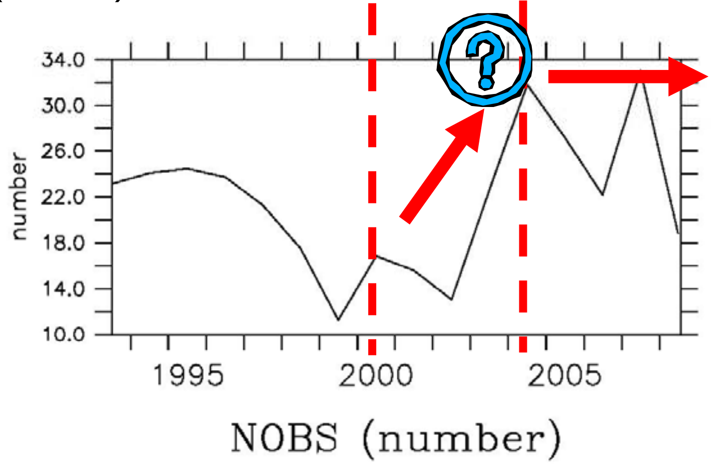

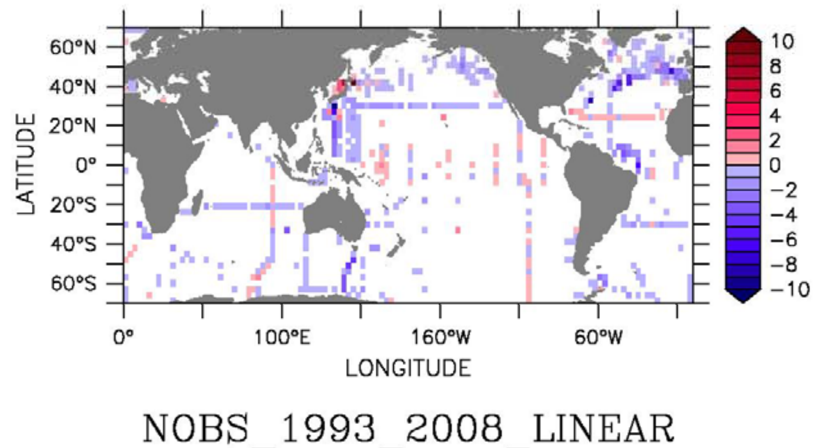

No significant relationship between two time series and spatial patterns.

There are very sparse datasets below 2000 m for 1993-2008, so we can not confirm any reliable trend.

Q2: HC700 is related to radiation flux of TOA ?

ΣQ=HC

HC/dt = Q

Q=0, flattening of HC

Q>0, increasing of HC

Q<0, decreasing of HC

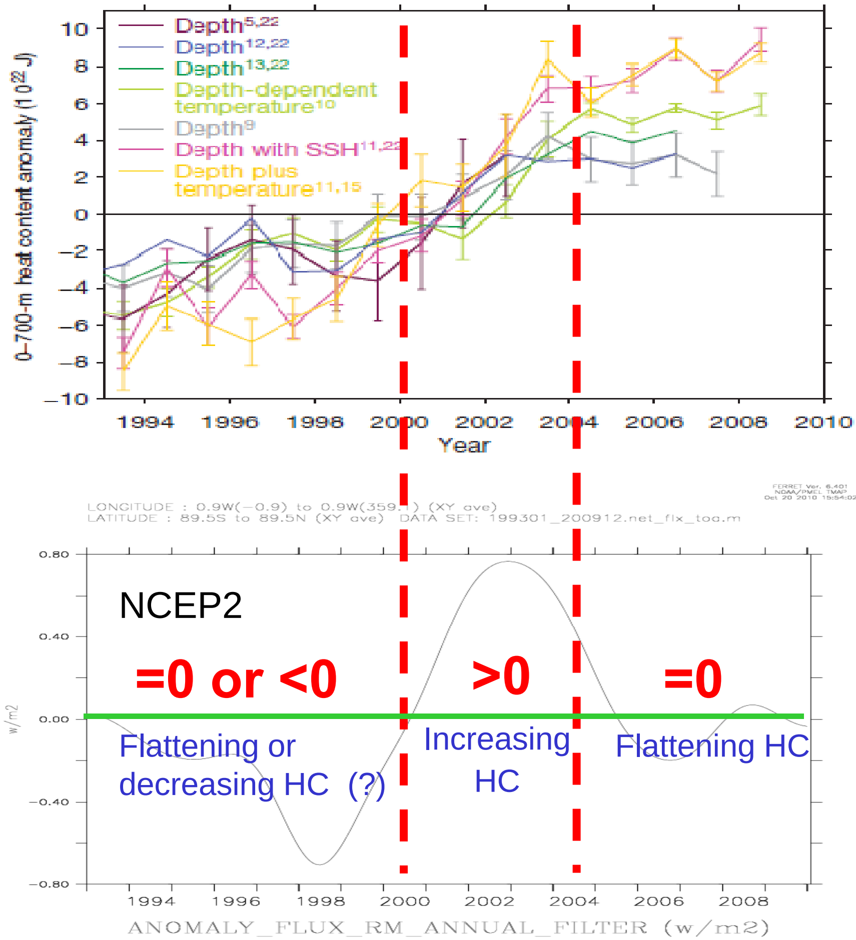

We calculate net heat flux (low pass filtering after annual cycle removed) at TOA from NCEP2 data. There is a reliable relationship between two curves especially after 2000, so we can conclude that the rapid increasing pattern is not a spurious due to any data sampling issue, but a real signal that is dynamically related to the radiation flux of TOA.

Q3: How is the spatial pattern of the heat content ?

Warming areas: Western Pacific, Atlantic, Indian Ocean…

Cooling areas: Eastern Pacific, Gulf stream path…

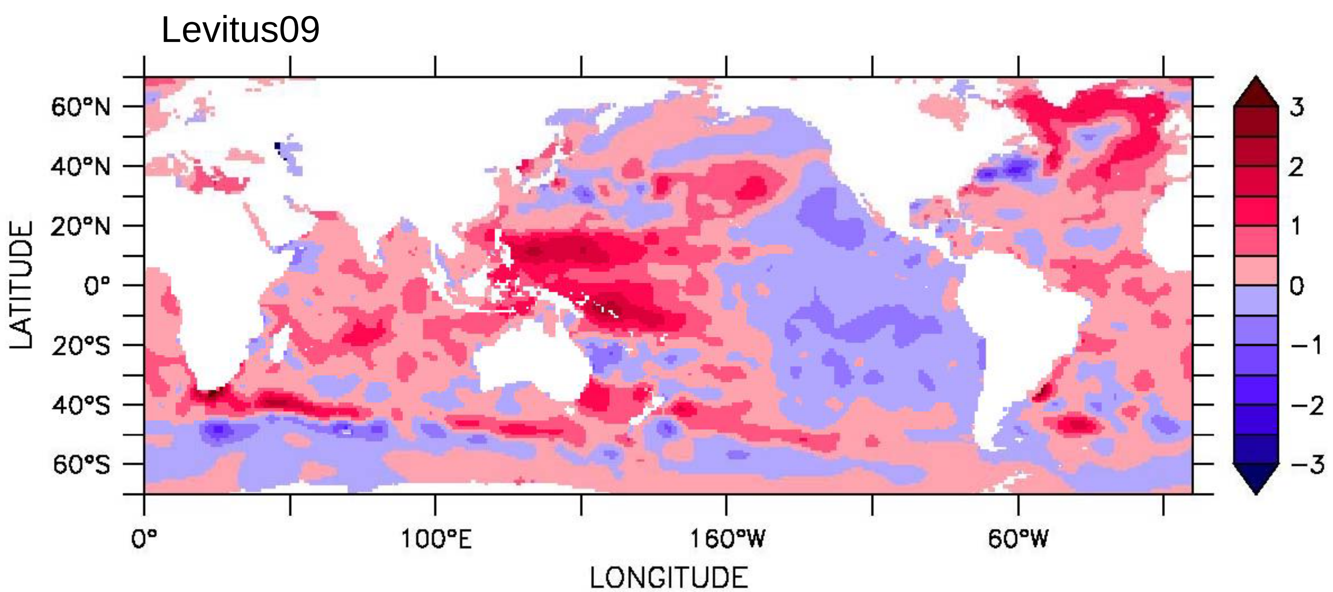

HC_1993_2009_LINEAR

The spatial pattern seems to be strongly related to the ENSO patterns.

So we have investigated the regional variability in HC700 by using EOF analysis.

EOF pattern of the HC700

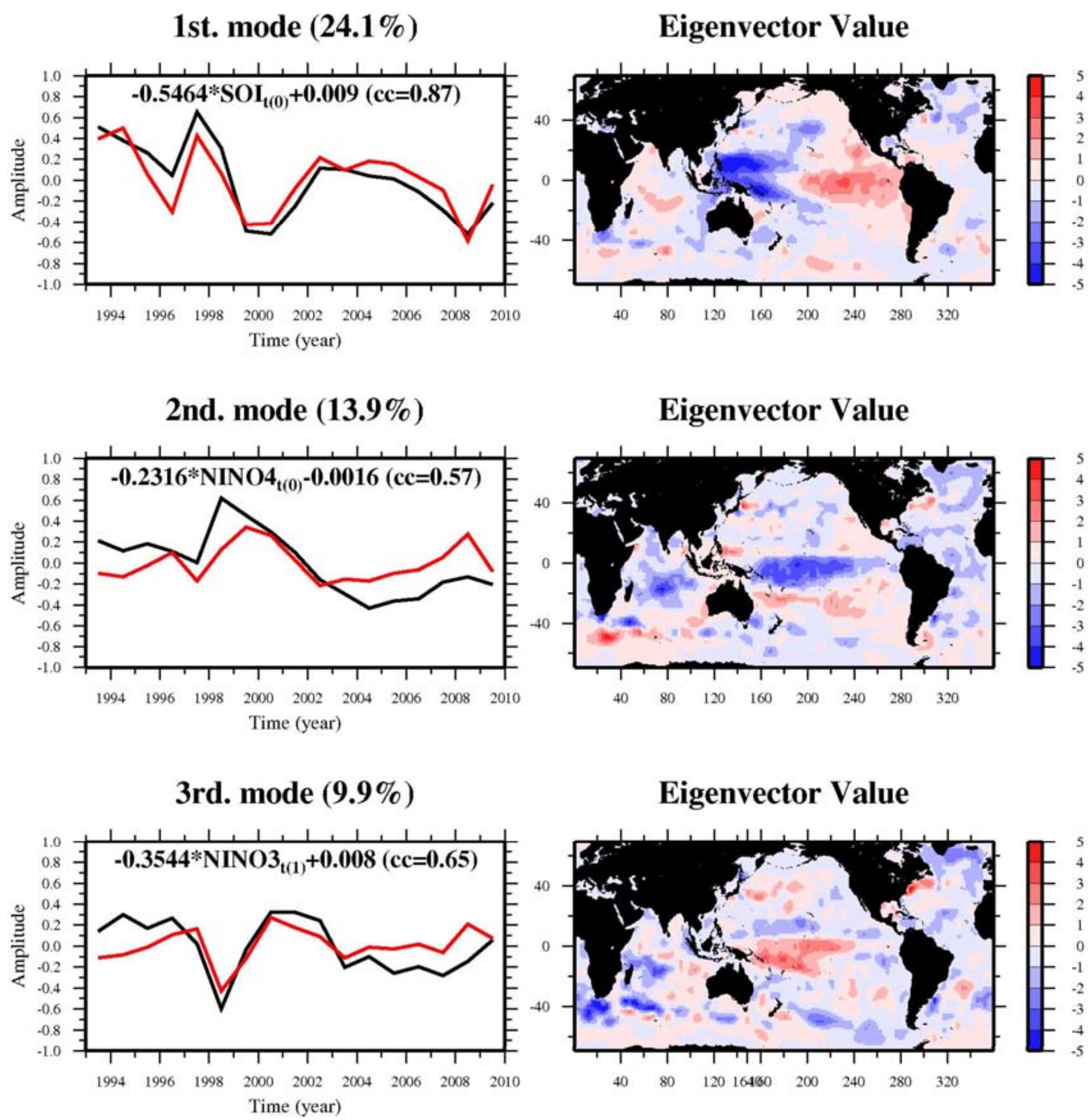

Black line: time series of each EOFs.

Red line: regression using Nino indices with time lag

EOF patterns of HC700 are strongly related to the ENSO patterns.

So, we attempt to remove ENSO signal from the gridded HC data.

We use traditional simple methods employing the linear regression into the dominant EOF time series with Nino indices (Kelly and Jones, 1996)

EOF series correlated with ENSO indices

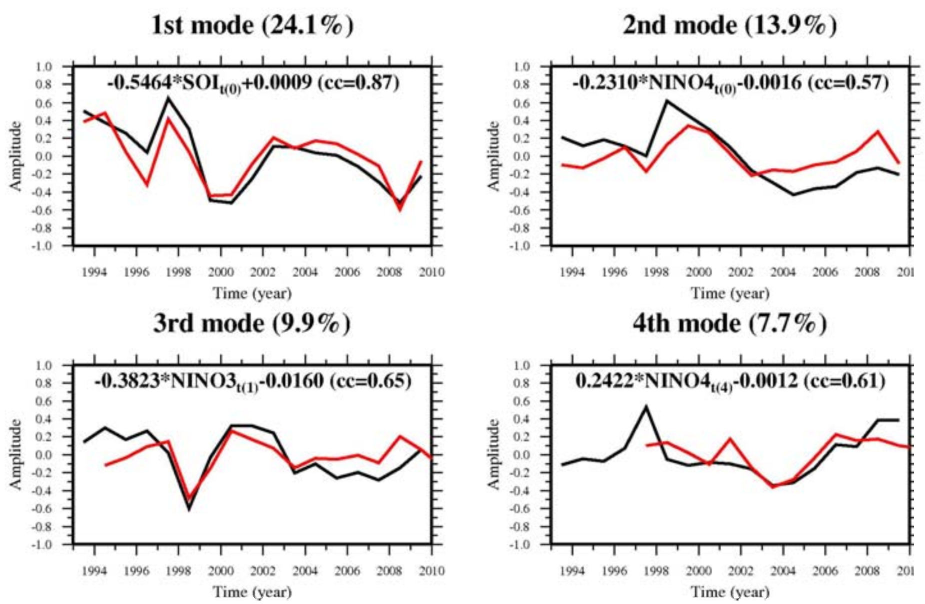

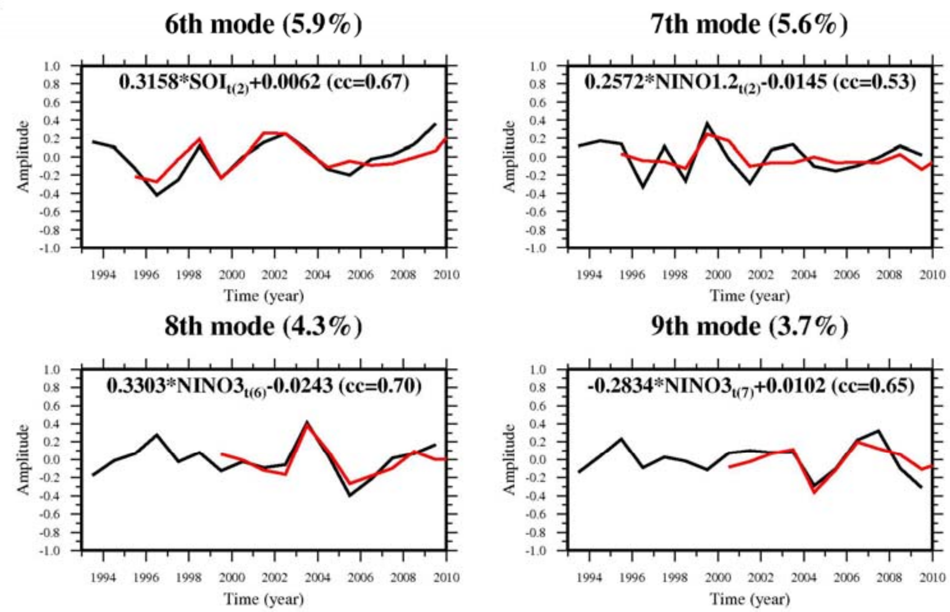

Black line: time series of each EOFs.

Red line: regression of selected Nino indices with time lag

We pick up 8 EOF series whose maximum correlation coefficients with selected Nino indices are more than 95% significant level.

Summary of the removal process

1. Calculate EOFs from HC700 raw data matrix.
   (EOF1(t)/w1(x,y), EOF2(t)/w2(x,y),…, EOF10(t)/w10(x,y))

2. Determine which EOFs are associated with the ENSO phenomenon by calculating the cross correlation coefficient (>95% sig. Level) between EOFs and five ENSO indices (SOI, Nino3, Nino4, Nino3.4, and Nino1+2)

3. Calculate the derived regression equation
   ENSO1(t) = -0.5464*SOI(t)+0.0009
   ENSO2(t) = -0.2310*NINO4(t)-0.0016
   ,……,
   ENSO8(t) = -0.2834*NINO3(t+7)+0.0102

4. Subtract the ENSO signal identified in the time series associated with EOFs.

   CHC (Corrected Heat Content) (x,y,t) =
   HC (x,y,t) - ENSO1(t)w1(x,y) - ENSO2(t)w2(x,y) - ENSO3(t)w3(x,y) – ENSO4(t)w4(x,y) - ENSO5(t)w6(x,y) - ENSO6(t)w7(x,y) - ENSO7(t)w8(x,y) - ENSO8(t)w9(x,y)

Reconstruct time series uncorrelated with ENSO

Black line: time series of raw data.

Red line: time series of reconstructed data uncorrelated with ENSO signal.

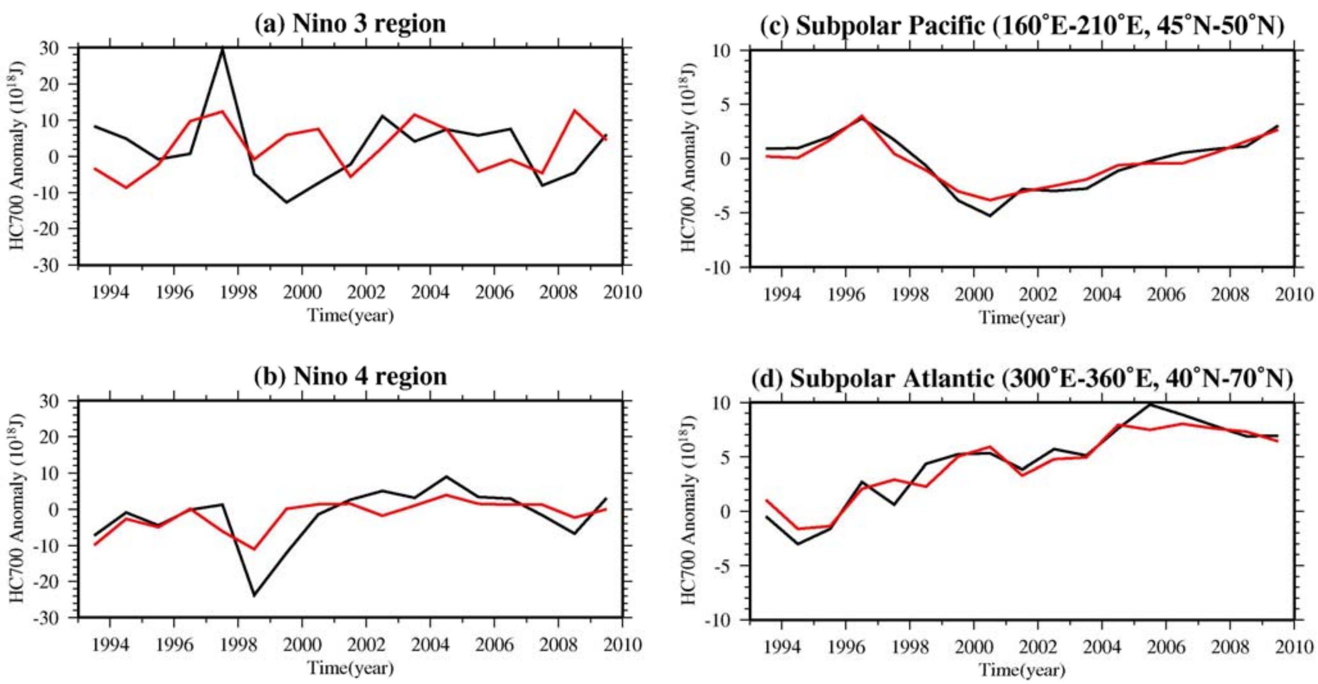

Strong interannual cycle has been reduced around the equatorial area where ENSO signals are dominant.

Around off-equatorial areas, reconstruct time series keep the variability which may not be related with ENSO phenomena.

EOF patterns uncorrelated with ENSO

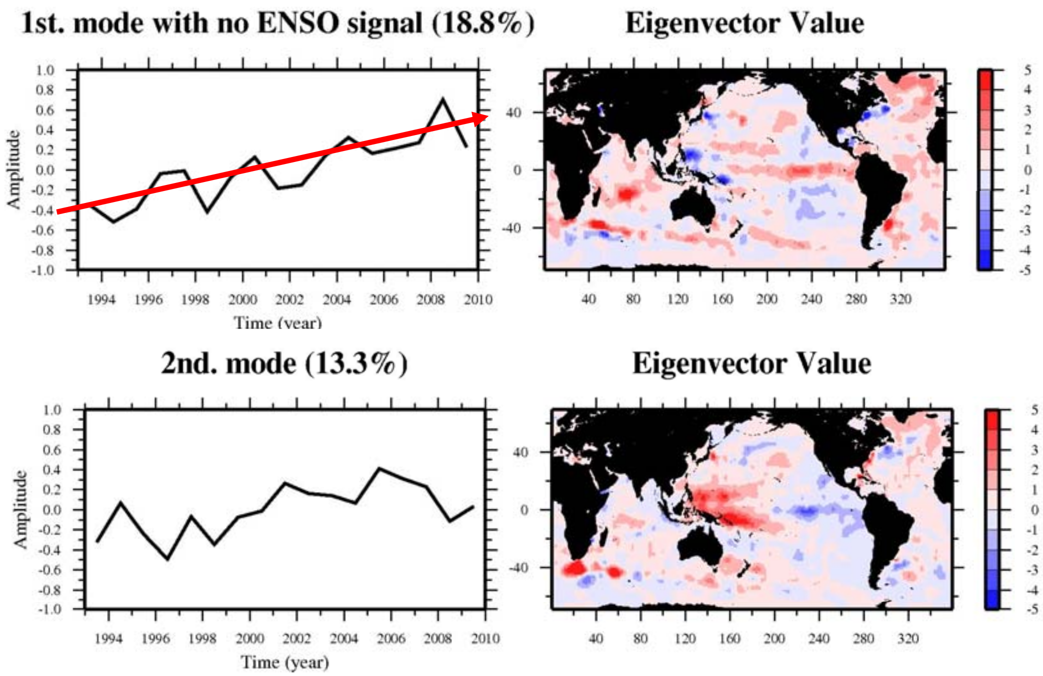

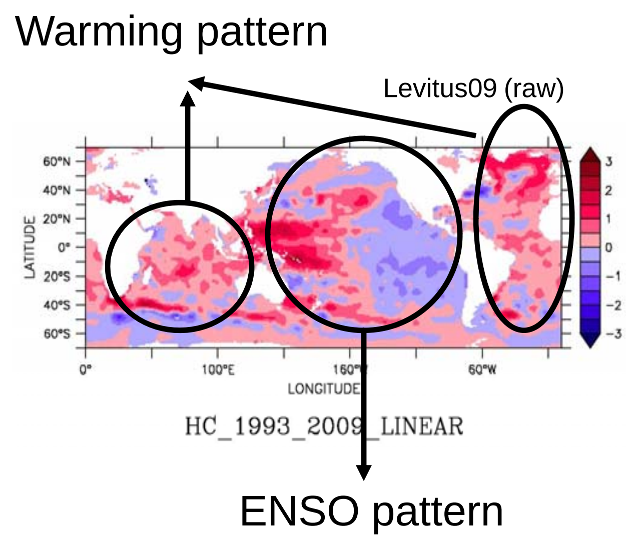

EOF 1st mode shows a stead warming trend. This warming pattern is shown in the Atlantic Ocean especially including subpolar gyre and Indian Ocean, which is very similar with the linear trend pattern of HC700 raw data.

In the 2nd mode, ENSO pattern around the Pacific Ocean still remained. There are possible limitations with the ENSO-removal method used in this study, which employs the linear regression on the time series of some ENSO index (ENSO-unrelated variations can occur in the ENSO index. ENSO-related variations occur in step around the globe. Observed ENSO evolution does not involve in just a couple of EOF patterns. ENSO has nonlinear characteristic…..) .

Q4: How is the deep ocean ?

Indian Ocean

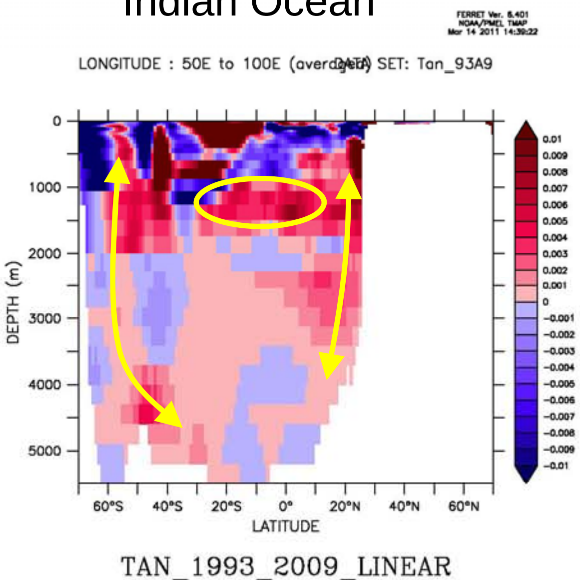

Pacific Ocean

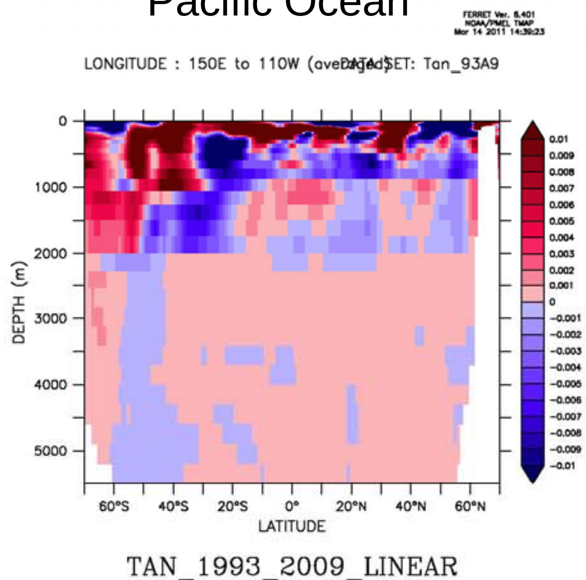

Atlantic Ocean

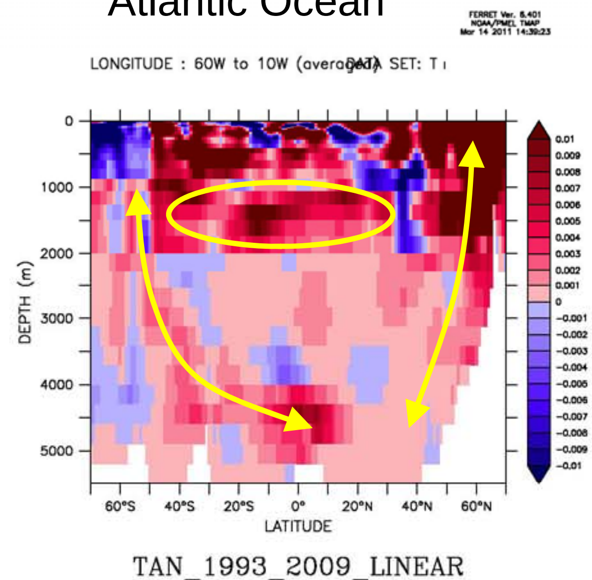

By using EN3 data, we investigate zonal mean temperature trend for 1993-2009 up to 5500 m depth.

In the Indian and Atlantic Ocean, we confirm significant warming trend below 1000 m and around the deep abyssal ocean, which may related to the upper ocean warming around these basins (Purkey and Johnson, 2010; Song and Colberg 2011).

Conclusion

Q1: HC700 is related to the different sampling era ?

The rapid increasing pattern of HC700 around 2000-2004 is not related to the number of data around the data transition periods from XBT to Argo.

Q2: HC700 is related to the radiation change of TOA ?

Rapid increasing pattern around 2000-2004 is associated with the radiation change of the top of atmosphere. They are dynamically related to each other and we confirmed it by using observation (reanalysis).

Q3: How is the spatial pattern of the heat content for 1993-2008?

Western Pacific, Atlantic, and Indian Oceans show significant warming trend during this period. When we remove ENSO signals, we obtain more stead warming trend as the 1^{st} EOF mode around the Atlantic and Indian Ocean.

Q4: How is the deep ocean ?

Deep ocean warming trend is found especially around the abyssal oceans of Atlantic and Indian Ocean, which may be related to the upper ocean warming.

Part 2: GFDL ECDA (Ensemble Coupled Data Assimilation System)

Model:

- Base model: GFDL CM2.1
- Assimilation scheme: Ensemble Kalman Filtering with cov(T,S)
- Initialization for 380 yrs from the 1860 fixed year radiative forcing run
- IPCC historical run with time varying GHGNA since 1861.
- Observed ocean profiles since 1976 with :
  - WOD09 (XBT, MBT, CTD, MRB, OSD)
  - Argo (2000-present)
  - GTSPP (2009-present)

Experiment:

- ECDA_full (1993-2006) (MBT, CTD, MRB, OSD, XBT, and Argo)
- ECDA_no_XBT (1993-2006) (MBT, CTD, MRB, OSD, and Argo)

GFDL ECDA

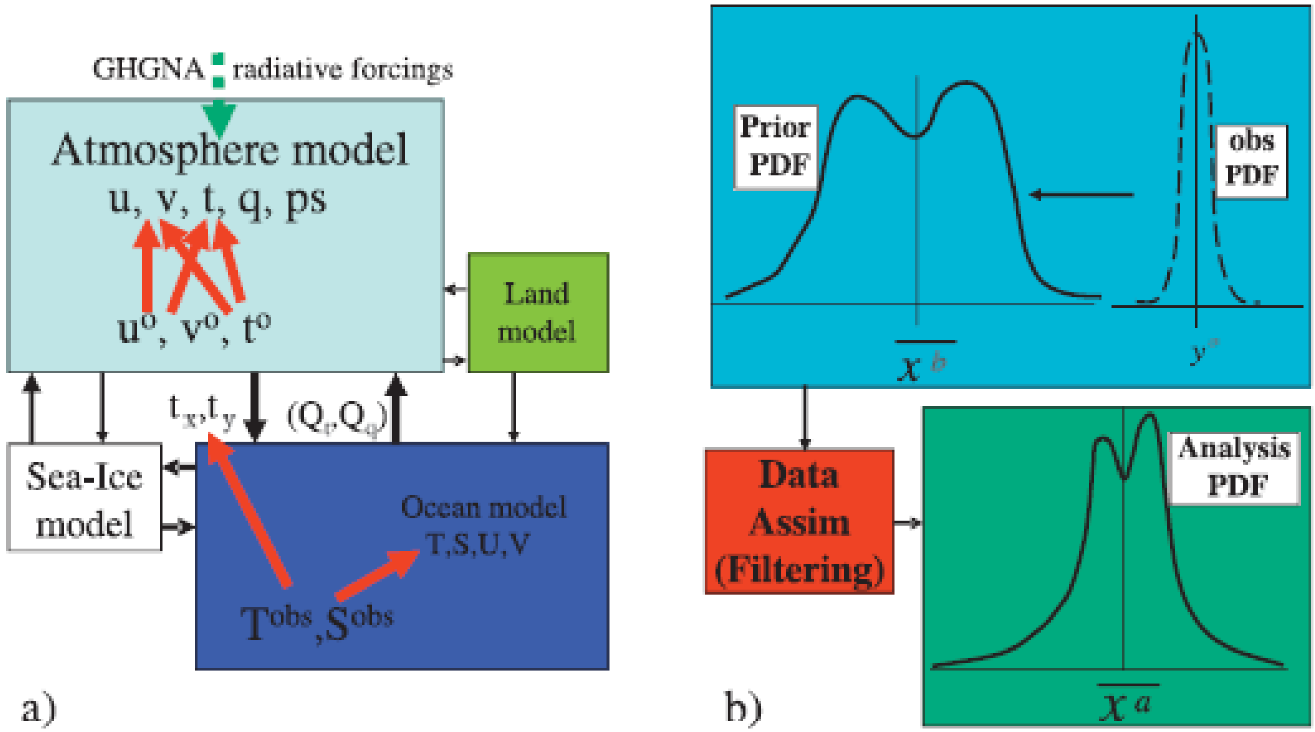

Cartoon of how (a) data assimilation (red arrow) in the GFDL coupled model transfers observational information into the coupled component by exchange fluxes (black arrows), and (b) an ensemble filter updates the probability distribution. [Zhang et al., 2007, 2010]

Oceanic data management system for ECDA

Step 1: Data Mirroring System (WOD09, Argo, GTSPP)

Step 2: Quality Control System (Real Time + Delayed Mode)

[QC Process, *Chang et al., (2009)*]

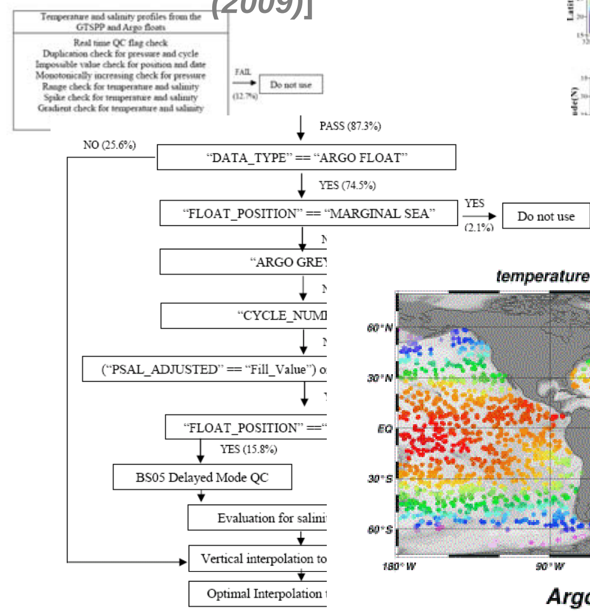

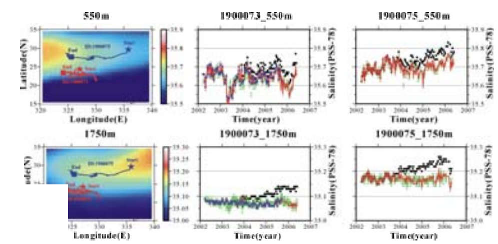

[DMQC result]

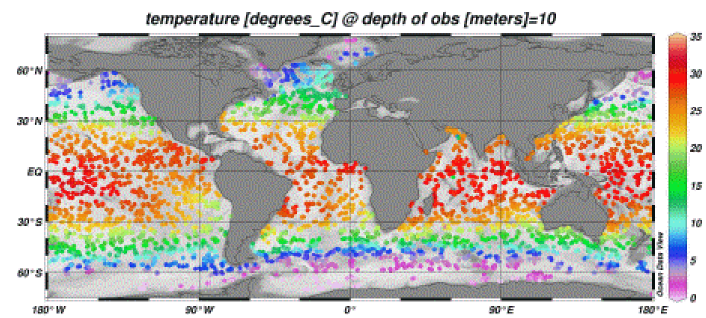

Argo in 01/2010 (QC by GFDL)

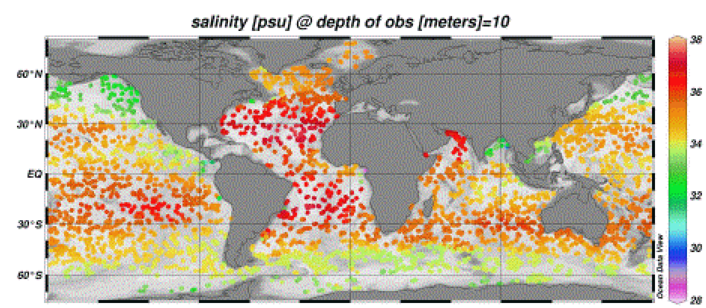

Step 3: Ensemble Coupled Data Assimilation System

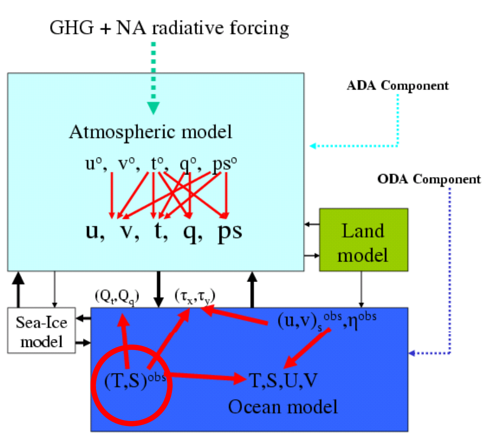

HC700 difference between ECDA_no_xbt and ECDA_full

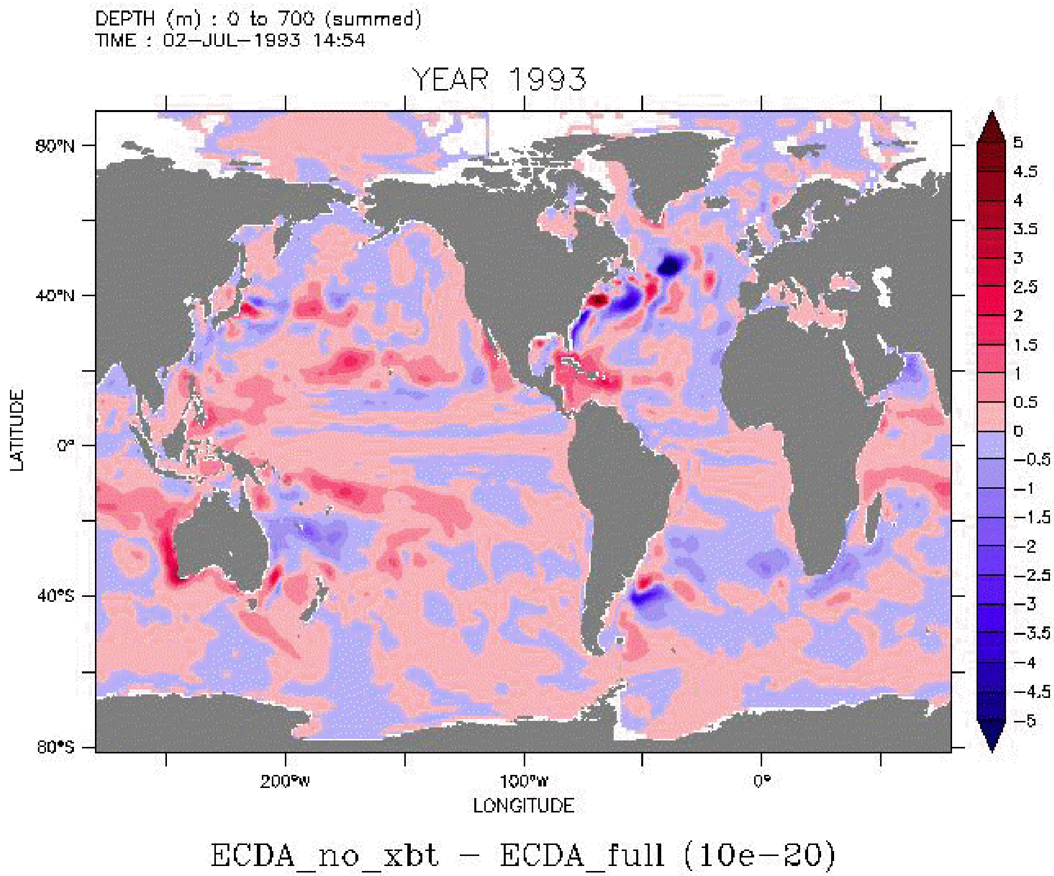

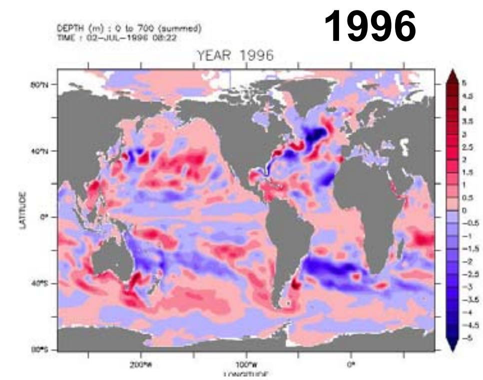

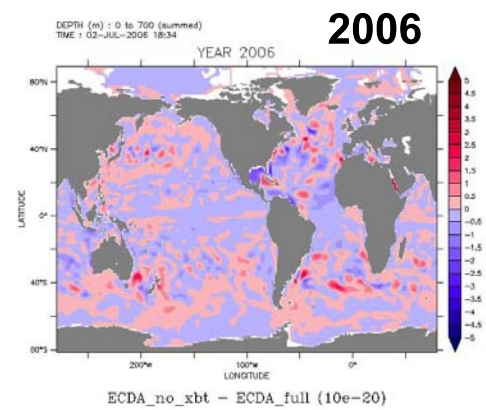

The XBT effect can be found globally especially along the ocean gyre systems.

There are also significant difference in the Southern Ocean

The difference is getting reduced in time.

RMSE change between ECDA_no_xbt and ECDA_full

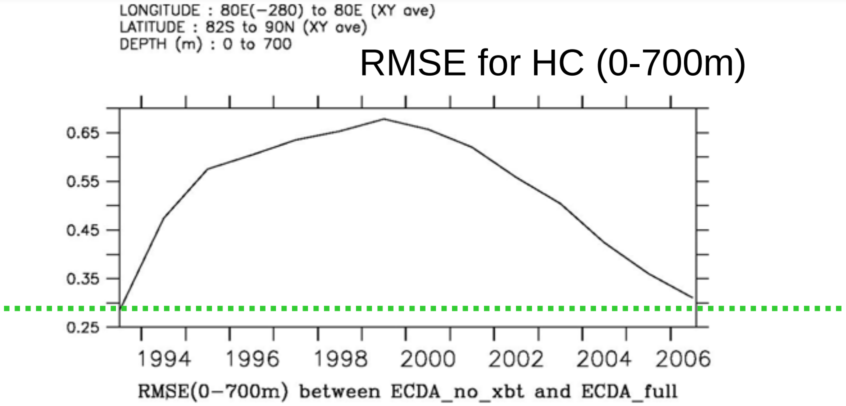

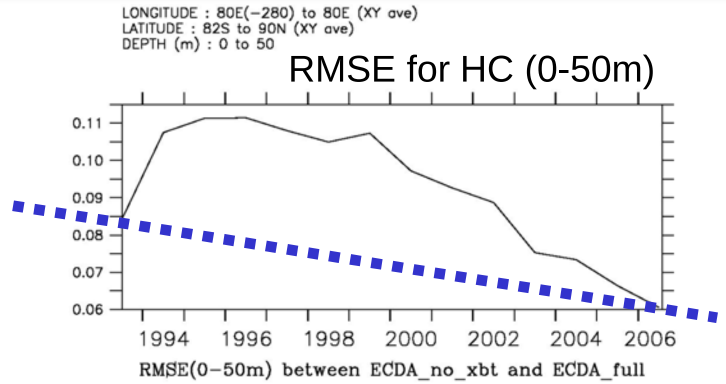

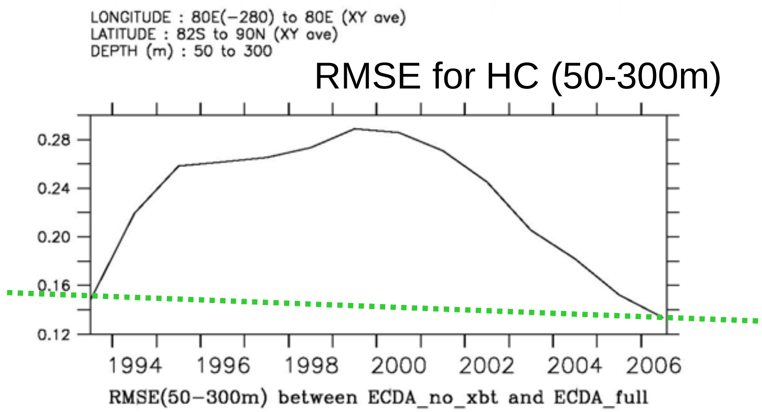

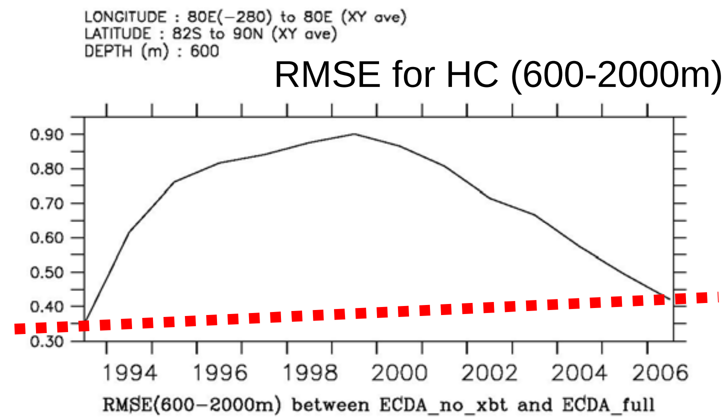

There are a little bit different patterns for RMSE change **in depth**.

Surface layer: XBT effects most rapidly decrease.

Subsurface layer below 600 m: XBT effect remains even after Argo periods.

Subsurface T,S change between ECDA_no_xbt and ECDA_full

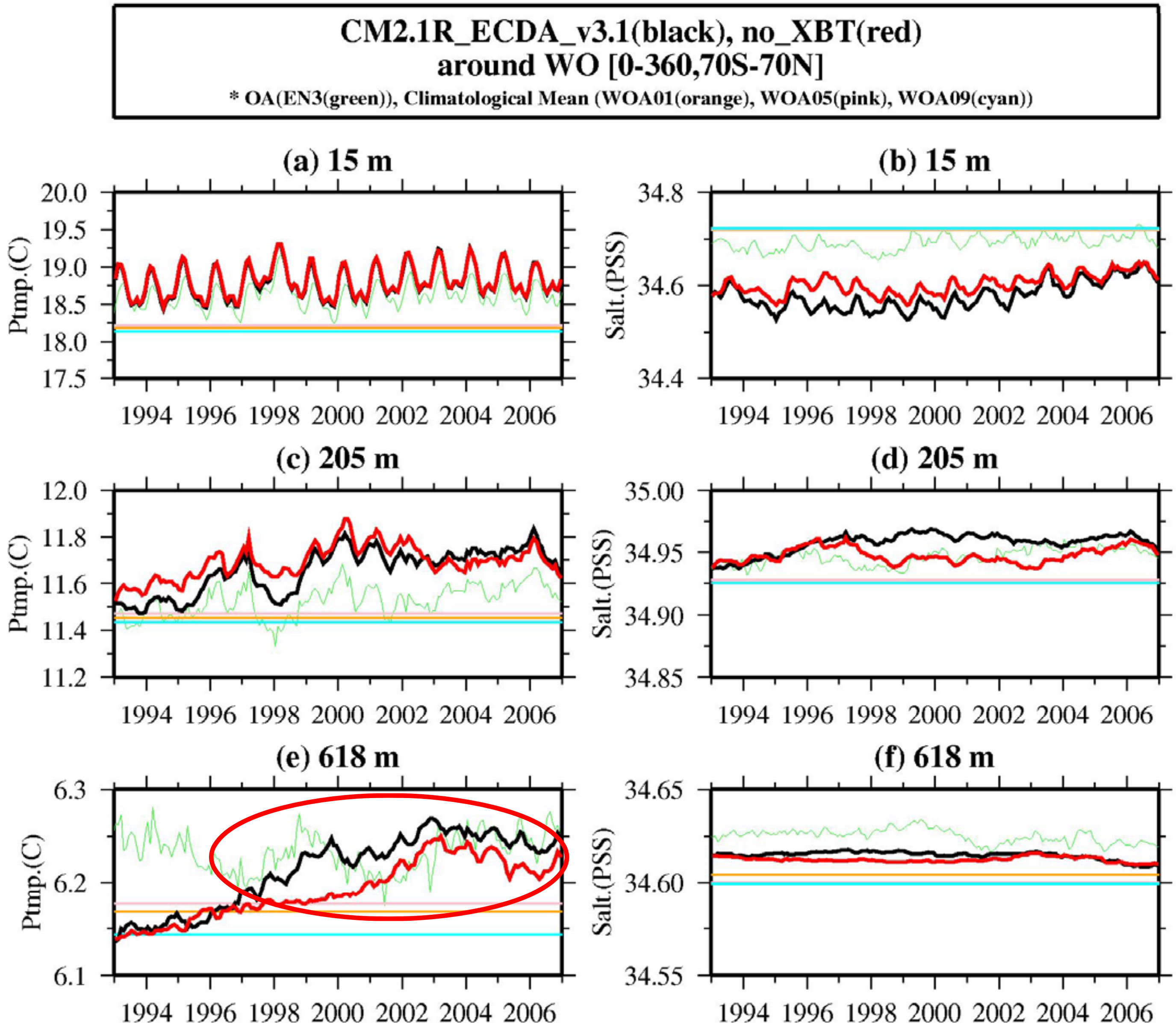

XBT affects the assimilated salinity field as well.

T/S difference reduced in time at 15 and 205m.

At 618m, the difference remains even after Argo period.

HC700 from observations and ECDA experiments

Levitus_2005 (gray), Levitus_2009 (black), EN3 (green)
ECDA_full (blue), ECDA_no_xbt (red)

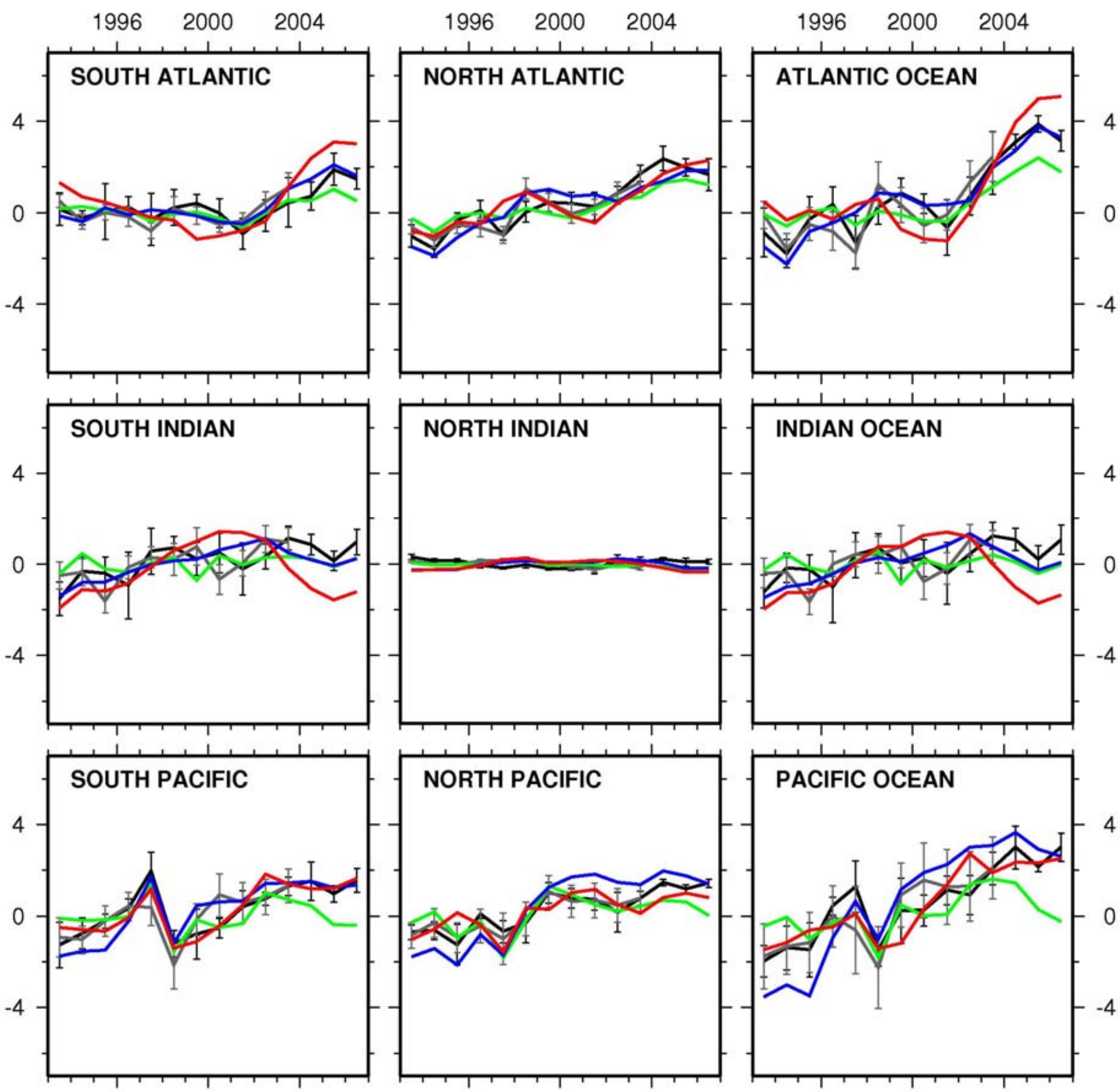

ECDA_no_xbt shows significant bias both for Atlantic and Indian Ocean.

ECDA_full shows bias in the Pacific, but variability is reasonable.

EN3 shows cold bias for Atlantic and Pacific during Argo periods.

XBT plays an important role for the HC simulation.

Conclusion

Q: How is the impact of XBTs on the GFDL's ensemble coupled data assimilation system.

We showed the XBT effects on the ECDA system

1. even in the Southern Oceans.

2. even after Argo periods especially for the subsurface depths.

3. even for salinity and other fields.

4. especially for the HC700 reanalysis around the Atlantic and Indian Oceans.

http://www.gfdl.noaa.gov/ocean-data-assimilation

Thank you !!
감사합니다 !!

Quality Control

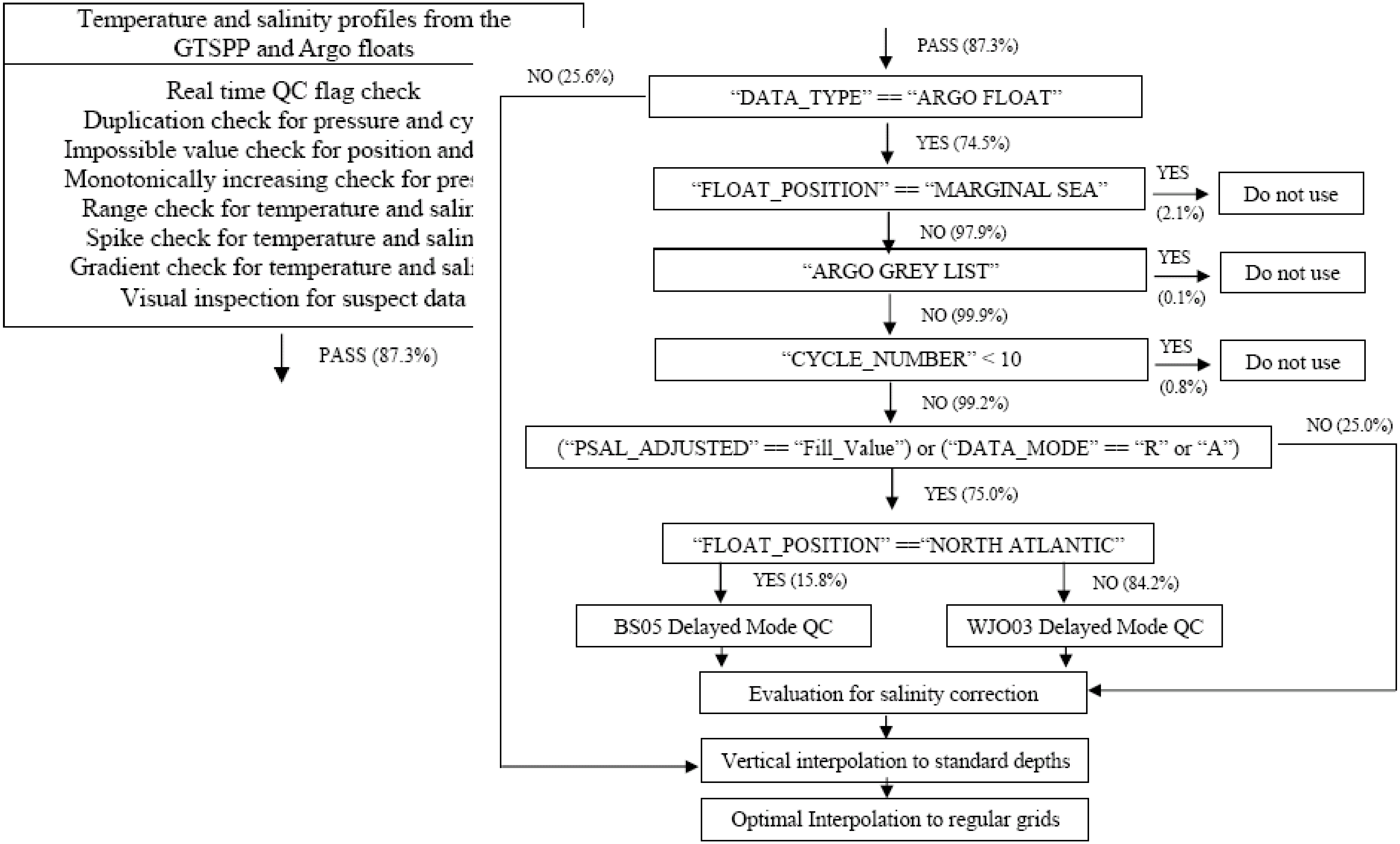

Quality Control [DMQC]

RTQC by DAC **DMQC by DAC** **Objective estimation** **DMQC by this study**

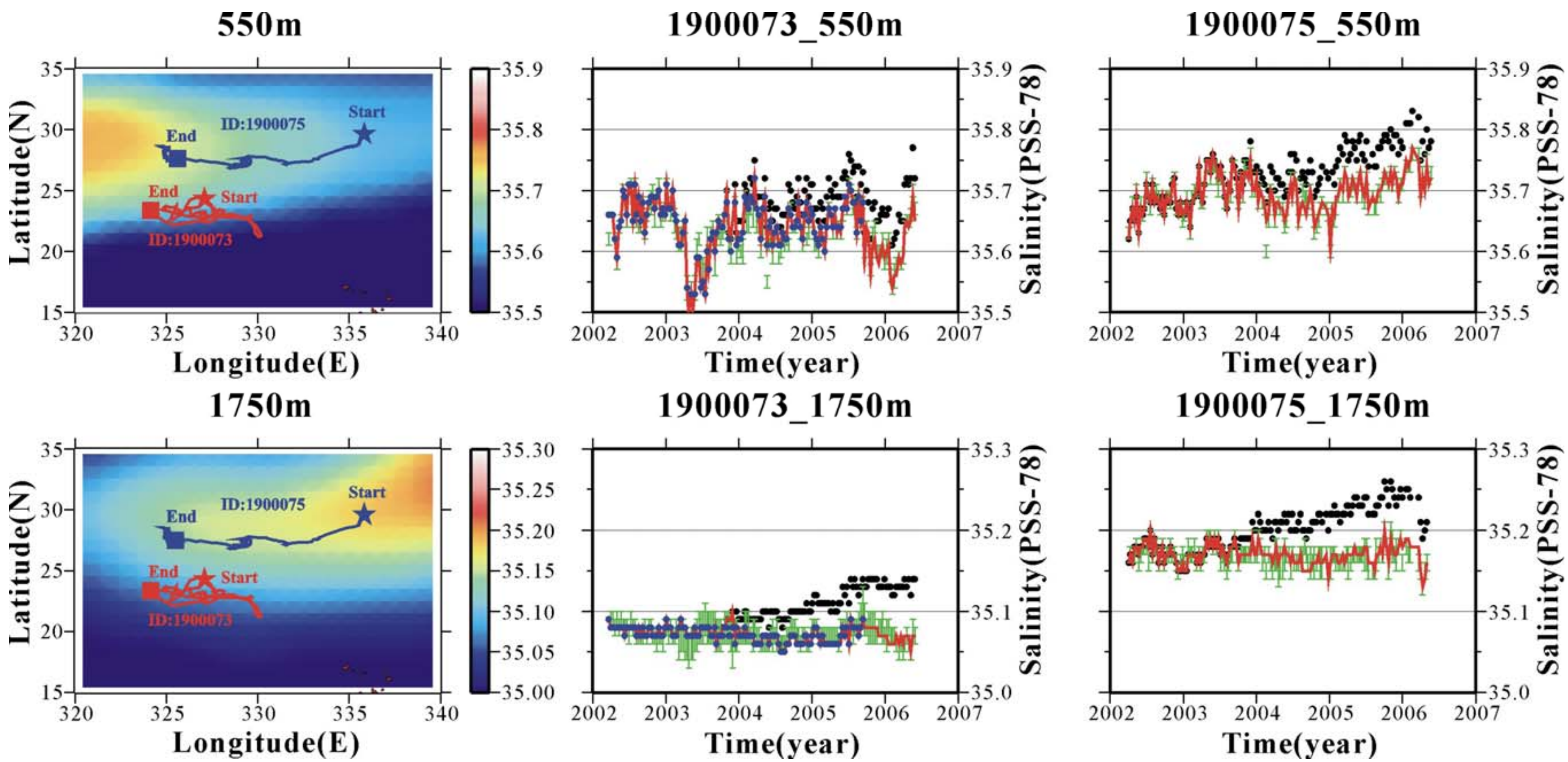

- Our calibrations are in line with climatology and DAC results.
- Many floats with salinity drift have not completed DMQC by DACs.

GFDL ECDA development